Effect of charge-density fluctuations on the order-disorder transition in the lattice restricted primitive models of electrolytes

A. Ciach
Institute of Physical Chemistry, Polish Academy of Sciences, 01-224 Warszawa, Poland
(Received 11 March 2004; revised manuscript received 23 June 2004; published 7 October 2004)

Lattice restricted primitive models, where equally charged ions of a diameter σ are located at sites of a simple cubic lattice with a lattice constant a, are studied within the field-theoretic approach. We focus on the transition between charge-disordered and charge-ordered phases for $\sigma/a=1$ and $\sigma/a=2$. By using renormalization-group methods we show that at high concentrations of ions the transition is continuous for $\sigma/a=1$, while for $\sigma/a=2$ it is only first order, as found previously in simulations. For $\sigma/a=1$ the effect of charge-density fluctuations on the positions of the continuous transition and the tricritical point (TCP) is determined within a formalism developed in this work. The temperature and the concentration of ions at the TCP agree very well with simulation results.

DOI: 10.1103/PhysRevE.70.046103 PACS number(s): 64.60.Cn, 05.10.Cc, 05.70.Jk

I. INTRODUCTION

Phase transitions and critical phenomena in ionic systems have been a subject of an intensive debate for many years. The simplest systems correspond to anions and cations having identical charges and very similar sizes. In the corresponding restricted primitive model (RPM) hard spheres of a diameter σ and charges $\pm e$ are immersed in a structureless solvent with a dielectric constant D. Experiments [1,2], simulations [3–8] and fluid theories (mean-spherical approximation [9,10] and extensions of the Debye-Hückel theory [11,12]) show coexistence between uniform ion-dilute and ion-dense phases with an associated critical point (CP) at low concentrations of ions, and crystallization at high concentrations. After long-lasting debate concerning the nature of criticality in the RPM, recent experiments [1], simulations [6,7] and field theory [13,14] all indicate that the critical point belongs to the Ising universality class. Unlike in simple fluids, however, the phase diagrams in the RPM depend on the space discretization σ/a when the ions are restricted to lattice sites on a simple cubic (sc) lattice with a lattice constant $a \leqslant \sigma$ [3,15–17]. For $\sigma/a=1$ only order-disorder transition between charge-disordered and charge-ordered phases (two oppositely charged sublattices) with an associated tricritical point (TCP) occurs; for $\sigma/a=2$ the order-disorder transition is only first order, i.e. the TCP disappears. For $\sigma/a \geqslant 3$ the phase diagram is of the same type as in continuum space.

Landau theory introduced in Ref. [13] predicts that only an order-disorder transition between charge-disordered and charge-ordered phases with an associated tricritical point (TCP) occurs. This result agrees with the RPM phase-behavior on the sc lattice, and is in a sharp qualitative disagreement with the phase diagram in continuum system. The failure of the Landau mean field (MF) theory in the continuum indicates particularly important role of fluctuations in ionic systems and a strong dependence of the role of fluctuations on space discretization. One should note that in the theories predicting correct topological structure of the phase diagram in the continuum RPM [9–12] the charge-correlations are partially included.

In this work we focus on qualitative and quantitative effects of fluctuations on phase transitions in the RPM in the framework of the field theory developed in Ref. [13]. There are two order parameters (OP) in the RPM: the local charge, $\phi(\mathbf{x})$, and number, $\rho(\mathbf{x})$, densities. Short-wavelength charge-density fluctuations dominate [18] and lead to the charge-ordered–charge-disordered phase transition. For different space discretizations σ/a this transition, continuous in MF, may become fluctuation-induced first-order [16,17]. The OP's are coupled beyond the Gaussian part of the functional, therefore in our theory also the ion-poor–ion-rich phase separation is found when the charge-density fluctuations are integrated out [13,14]. Here we shall focus only on the order-disorder transition.

Systematic study of the effect of the charge-density fluctuations on phase diagrams for different values of σ/a was begun in Ref. [16] in an approach following the Brazovskii theory [19]. According to the Landau-Brazovskii theory, when at the spinodal $\mathcal{G}=\int_{\mathbf{k}} \tilde{G}_{\phi\phi}(\mathbf{k}) \to \infty$, where $\tilde{G}_{\phi\phi}(\mathbf{k})$ is the OP correlation function in Fourier representation, the order-disorder transition is fluctuation-induced first-order, although MF predicts a continuous transition. It turns out that in continuum, on the fcc lattice and in model I (excluded simultaneous occupancy of the nearest-neighbor sites), $\mathcal{G}$ diverges at the spinodal [16,17], i.e., the transition is fluctuation-induced first-order. For $\sigma/a=1$ as well as for $\sigma/a=2$, $\mathcal{G}$ is finite. Simulations, however show continuous transition for $\sigma/a=1$, and first order transition for $\sigma/a=2$. In this work we consider the sc lattice with $\sigma/a=1$ (denoted by "sc") and $\sigma/a=2$ (denoted by "model III" after Ref. [16]). Using the renormalization-group (RG) method we present convincing arguments that the transition is continuous (at high temperatures) and first-order in the first and in the second model respectively.

The effect of fluctuations on the position of the λ-line in the case of the sc lattice has been studied in Ref. [20] within Debye-Hückel (DH) theory and in Ref. [21] within hierarchical reference theory (HRT). In the case of the DH theory the temperature at the TCP deviates from the result of simulations [3,4] by more than 100%. In the second theory the

accuracy is better, i.e., for the temperature at the TCP the relative difference from the simulation result is ~30%. In this work we determine the shift of the line of continuous order-disorder transitions (λ-line) on the sc lattice within the field-theory developed in Ref. [13]. The shifts of temperature and density at the TCP and along the λ-line are obtained by using the self-consistent Hartree approximation and the weighted field theory [13], respectively. The results agree very well with simulations.

In Sec. II the models with $\sigma/a=1$ (sc) and $\sigma/a=2$ (model III) are introduced and the MF theory is briefly described. In Sec. III the weighted field approximation is developed. Section IV contains the analysis of the effects of charge-density fluctuations on the order of the charge-ordered–charge-disordered transition in the two models. The position of the λ-line for $\sigma/a=1$ is found in Sec. V. Section VI contains a short summary.

II. THE MODELS AND THE MEAN-FIELD APPROXIMATION

The Hamiltonian of the lattice restricted primitive model (LRPM) in the general case of ions that can have extended cores on the sc lattice is given by [16]

$$H=\frac{E_0}{2}\sum_{\mathbf{x}}\sum_{\mathbf{x}'}V(|\mathbf{x}-\mathbf{x}'|)\hat{s}(\mathbf{x})\hat{s}(\mathbf{x}'), \tag{1}$$

where $\hat{s}=+1,-1,0$ represents the anion, the cation and the solvent (or vaccum in the case of molten salts), respectively. The lattice sites are $\mathbf{x}=x_i\mathbf{e}^i$, where $\mathbf{e}^i$ are the unit lattice vectors, x_i are integer numbers, $i=1,2,3$, summation convention is used and the distance is measured in a units. The energy unit is $E_0=e^2a_{nn}^2/Dv_0$, where D is the dielectric constant of the solvent, a_{nn} is the distance between nearest-neighbor sites and v_0 is the volume per lattice site [20]. The corresponding dimensionless temperature is $T^E=1/\beta^E=kT/E_0$. $T^E=T^*$ for $\sigma/a=1$, where $T^*=kTD\sigma/e^2$ is the standard reduced temperature. Finally,

$$V(|\Delta\mathbf{x}|)=g(|\Delta\mathbf{x}|)V_c(|\Delta\mathbf{x}|), \tag{2}$$

where $V_c(|\mathbf{x}-\mathbf{x}'|)$ is the dimensionless Coulomb potential on the sc lattice (see the Appendix) and the form of $g(|\mathbf{x}-\mathbf{x}'|)$ follows from the requirement that the contribution to the electrostatic energy from ions occupying forbidden pairs of sites is not included in Eq. (1). Hence for both considered models we assume $g(|\Delta\mathbf{x}|)=0$ for $|\Delta\mathbf{x}|$ smaller than the ion diameter, and $g(|\Delta\mathbf{x}|)=1$ for $|\Delta\mathbf{x}|\geqslant\sigma$. The explicit form of g for $\sigma/a=1$ is thus

$$g^{sc}(|\Delta\mathbf{x}|)=1-\delta^{Kr}(|\Delta\mathbf{x}|). \tag{3}$$

In model III the sites inside the $3\times3\times3$ cube cannot be occupied simultaneously with the central site of this cube, therefore for model III we have

$$g^{\mathrm{III}}(|\Delta\mathbf{x}|)=1-\delta^{Kr}(|\Delta\mathbf{x}|)-\sum_i\delta^{Kr}(|\Delta\mathbf{x}\pm\mathbf{e}_i|)-\sum_{i<j}\delta^{Kr}(|\Delta\mathbf{x}\pm\mathbf{e}_i\pm\mathbf{e}_j|)-\delta^{Kr}(|\Delta\mathbf{x}\pm\mathbf{e}_1\pm\mathbf{e}_2\pm\mathbf{e}_3|). \tag{4}$$

In Fourier representation we obtain the following forms of the potential $\tilde{V}$ in the two considered cases:

$$\tilde{V}^{sc}(\mathbf{k})=\tilde{V}_c(\mathbf{k})-2\pi V_0^{sc}\quad(\mathrm{sc}) \tag{5}$$

and

$$\tilde{V}^{\mathrm{III}}(\mathbf{k})=\tilde{V}_c(\mathbf{k})-2\pi[V_0^{sc}+6V_1^{sc}\tilde{f}_{sc}(\mathbf{k})+12V_2^{sc}\tilde{f}_{fcc}(\mathbf{k})+8V_3^{sc}\tilde{f}_{bcc}(\mathbf{k})]\quad(\text{model III}). \tag{6}$$

The lattice Coulomb potential $\tilde{V}_c(\mathbf{k})$, the lattice characteristic functions $\tilde{f}_{latt}(\mathbf{k})$ and the constants V_n^{sc} for $n=0-3$ are given in the Appendix.

We consider an open system with equal chemical potentials of the two ionic species, $\mu_+=\mu_-$. Thus, in the case of molten salts only one chemical potential is independent. Because of close packing (each site is occupied either by an ion or by a solvent molecule), also in the case of solutions there is only one independent chemical potential. The natural choice is $\mu=1/2(\mu_++\mu_-)-\mu_0$, i.e., the chemical potential difference between the solute $\mu_+=\mu_-$ and the solvent, μ_0 (for molten salts we assume the same μ with $\mu_0=0$). The microstates with overlapping hard spheres, i.e., $\{\hat{s}(\mathbf{x})\}$ such that there exist $\mathbf{x}$ and $\Delta\mathbf{x}\neq0$ for which $\hat{s}(\mathbf{x})\hat{s}(\mathbf{x}+\Delta\mathbf{x})(1-g(\Delta\mathbf{x}))\neq0$, are excluded. Only ions cannot overlap in this model (the solvent is "structureless"). The probability of the allowed microscopic state $\{\hat{s}(\mathbf{x})\}$ is

$$p[\{\hat{s}(\mathbf{x})\}]=\Xi^{-1}\exp[-\beta(H[\{\hat{s}(\mathbf{x})\}]-\mu\sum_{\mathbf{x}}\hat{s}^2(\mathbf{x}))]. \tag{7}$$

In the above $\Xi=\Sigma_{\{\hat{s}(\mathbf{x})\}}\exp[-\beta(H[\{\hat{s}(\mathbf{x})\}]-\mu\Sigma_{\mathbf{x}}\hat{s}^2(\mathbf{x}))]$, where $\Sigma_{\{\hat{s}(\mathbf{x})\}}$ means summation over allowed microstates. Thermodynamics is determined by the grand thermodynamic potential $\Omega=-kT\log\Xi$. The symmetry of Eq. (7) with respect to $\hat{s}\to-\hat{s}$ leads to $\langle\hat{s}\rangle=0$. Note, however that for oppositely charged nearest neighbors the Hamiltonian (1) assumes very low negative values. In contrast, the Hamiltonian assumes very large, positive values when $\hat{s}(\mathbf{x})>0$ [or $\hat{s}(\mathbf{x})<0$] for $\mathbf{x}$ belonging to a large, coherent region. As a consequence, spontaneous symmetry breaking, $\langle\hat{s}(\mathbf{x})\rangle\neq0$, is associated with violations of the charge neutrality in microscopic regions (neighboring regions being oppositely charged). Moreover, in thermodynamic limit global charge neutrality $[\Sigma_{\mathbf{x}}\langle\hat{s}(\mathbf{x})\rangle=0]$ should be obeyed.

In the MF approximation the average charge and number densities are identified with the most probable values, ϕ_0,ρ_0. These fields correspond to a global minimum of the grand-potential functional in the MF approximation

$$\beta\Omega^{MF}[\phi,\rho] = \beta F_{hs}[\phi,\rho] + \beta U[\phi] - \beta\mu\sum_{\mathbf{x}} \rho(\mathbf{x}), \quad (8)$$

where $F_{hs}[\phi,\rho]$ is the free energy of the uncharged reference system. For $\sigma/a=1$ it has the form of the ideal entropy of mixing,

$$\beta F_{hs}[\phi,\rho] = \sum_{\mathbf{x}} \left[\frac{\rho+\phi}{2} \log\left(\frac{\rho+\phi}{2}\right) + \frac{\rho-\phi}{2} \log\left(\frac{\rho-\phi}{2}\right) + (1-\rho)\log(1-\rho) \right]. \quad (9)$$

In model III $F_{hs}[\phi,\rho]$ assumes a different form. However, the order of the order-disorder transition is independent of the form of $F_{hs}[\phi,\rho]$, as will be shown later.

The electrostatic energy $U[\phi]$ in Fourier representation is given by

$$U[\phi] = \frac{E_0}{2} \int_{\mathbf{k}} \tilde{V}(\mathbf{k}) \tilde{\phi}(\mathbf{k}) \tilde{\phi}(-\mathbf{k}), \quad (10)$$

where $\tilde{V}(\mathbf{k})$ is given in Eqs. (5) and (6) for the two models, $\mathbf{k}=(k_1,k_2,k_3)$ and we use the notation

$$\int_{\mathbf{k}} \equiv \int_{-\pi}^{\pi} \frac{dk_1}{2\pi} \int_{-\pi}^{\pi} \frac{dk_2}{2\pi} \int_{-\pi}^{\pi} \frac{dk_3}{2\pi}. \quad (11)$$

The charge and number densities ϕ and ρ are dimensionless; the average dimensionless-density ρ is the fraction of ion-occupied sites.

Ω^{MF} given in Eq. (8) can be expanded about its minimum at $\phi(\mathbf{x})=0$, $\rho(\mathbf{x})=\rho_0$. The expansion in ϕ and $\Delta\rho=\rho-\rho_0$ has the form

$$\begin{aligned}\Omega^{MF}[\phi,\rho] = \Omega^{MF}[0,\rho_0] &+ \frac{1}{2}\sum_{\mathbf{x}_1}\sum_{\mathbf{x}_2} C^0_{\phi\phi}(\mathbf{x}_1,\mathbf{x}_2)\phi(\mathbf{x}_1)\phi(\mathbf{x}_2) \\ &+ \frac{1}{2}\sum_{\mathbf{x}_1}\sum_{\mathbf{x}_2} C^0_{\rho\rho}(\mathbf{x}_1,\mathbf{x}_2)\Delta\rho(\mathbf{x}_1)\Delta\rho(\mathbf{x}_2) \\ &+ \sum_{m>1,n>2} \sum_{\mathbf{r}_1} \cdots \sum_{\mathbf{r}_{2m}} \sum_{\mathbf{x}_1} \cdots \sum_{\mathbf{x}_n} \frac{\gamma_{2m,n}}{(2m)!\,n!} \\ &\times \phi(\mathbf{r}_1)\cdots\phi(\mathbf{r}_{2m})\Delta\rho(\mathbf{x}_1)\cdots\Delta\rho(\mathbf{x}_n), \end{aligned} \quad (12)$$

where $\gamma_{2m,n}$, given by respective derivatives of Ω^{MF} at $\phi=0,\rho=\rho_0$, are functions of ρ_0. Following the density-functional theory [22], the charge-charge and number-number correlation functions $G^0_{\phi\phi}$ and $G^0_{\rho\rho}$ are defined as inverse (in the matrix sense) to the second functional derivatives of $\beta\Omega^{MF}$. In Fourier representation we thus have the following forms of the correlation functions in the uniform phase ($\phi=0$, $\rho=\rho_0$) [13]

$$\tilde{G}^{0-1}_{\phi\phi}(\mathbf{k}) = \tilde{C}^0_{\phi\phi}(\mathbf{k}) = \frac{\delta^2\beta\Omega^{MF}}{\delta\tilde{\phi}(\mathbf{k})\delta\tilde{\phi}(-\mathbf{k})} = \rho_0^{-1} + \beta^E\tilde{V}(\mathbf{k}) \quad (13)$$

and

$$\tilde{G}^{0-1}_{\rho\rho}(\mathbf{k}) = \tilde{C}^0_{\rho\rho}(\mathbf{k}) = \frac{\delta^2\beta\Omega^{MF}}{\delta\tilde{\rho}(\mathbf{k})\delta\tilde{\rho}(-\mathbf{k})} = \frac{\delta^2\beta F_{hs}}{\delta\tilde{\rho}(\mathbf{k})\delta\tilde{\rho}(-\mathbf{k})} > 0, \quad (14)$$

respectively. $\tilde{C}^0_{\rho\rho}>0$, therefore there is no transition between two fluid phases on the MF level. The continuous transition to the charge-ordered phase is given by $\rho_0^{-1}+\beta^E\tilde{V}(\mathbf{k}_b)=0$ where at $\mathbf{k}=\mathbf{k}_b$, $\tilde{V}(\mathbf{k})$ assumes a minimum. The instability of the uniform phase is induced by dominant fluctuations $\phi(\mathbf{x})=\Phi\cos(\mathbf{x}\cdot\mathbf{k}_b)$, which correspond to the largest decrease of the electrostatic energy for a given amplitude Φ of the charge-wave.

For $\sigma/a=1$, $\mathbf{k}_b=\pi(\pm1,\pm1,\pm1)$ [13,15], whereas in model III the potential (6) assumes a minimum at $\cos k_i=z$ for $i=1,2,3$, where z satisfies the equation

$$\frac{1}{9(1-z)^2} = 2V_1^{sc} + 8V_2^{sc}z + 8V_3^{sc}z^2. \quad (15)$$

We find $z\approx0.708$, which is close to $\cos(\pi/4)$. The bifurcation vector is thus $\mathbf{k}_b=k_b(\pm1,\pm1,\pm1)$, where our simple approximation gives $k_b\approx\pi/4$. The order-disorder transition line is

$$S = S_\lambda^{MF}, \quad (16)$$

where

$$S = T^E/\rho_0, \quad S_\lambda^{MF} = -\tilde{V}(\mathbf{k}_b). \quad (17)$$

For $\sigma/a=1$, $S_\lambda^{MF}\approx2.13$ [13,15] and in model III we find $S_\lambda^{MF}\approx3.2$. The continuous transition to the charge-ordered phase, predicted by the above MF approximation, indeed occurs for $\sigma/a=1$ [3,20,21]. However, the MF value of S at the λ-line, and consequently the temperature at the TCP, $T^E_{tc}\approx0.7$ [15], are significantly overestimated, compared to the simulation results $T^E_{tc}\approx0.14$ (Ref. [4]) and $T^E_{tc}\approx0.15$ (Ref. [3]). Only first-order transition was found for model III in simulations [3].

III. FIELD THEORY FOR THE LRPM

A. Fundamentals

The field-theoretic approach to the RPM closely follows the theory developed for a description of critical phenomena in simple and complex fluids. Instead of considering microscopic states $\{\hat{s}(\mathbf{x})\}$, we consider smooth order-parameter (OP) fields (functions in the lattice case) within a coarse-grained description [23]. Such description is justified when the instability of the disordered phase is induced by small-amplitude fluctuations, i.e., for continuous or weakly first-order transitions. The formalism described below is quite general, except that the explicit forms of the coupling constants depend on the model. The coupling constants are needed for a determination of quantitative effects of fluctuations. Only for $\sigma/a=1$ the quantitative effects are studied, and only for this model the explicit forms of the coupling constants will be given.

According to the fluctuation theory of Landau, the fluctuations $\phi(\mathbf{x})$ and $\rho(\mathbf{x})$ are excited with a probability deter-

mined by the corresponding increase of the grand thermodynamic potential. We therefore postulate that in an open system the probability of $\phi(\mathbf{x})$ and $\rho(\mathbf{x})$ is proportional to $\exp(-\beta\Omega^{MF})$. Following the standard procedure we introduce spatially varying external fields (sources) $\overline{\mu}(\mathbf{x}) = \mu + \Delta\mu(\mathbf{x})$ and $J(\mathbf{x})$, and the functionals of them

$$\Xi[J(\mathbf{x}),\overline{\mu}(\mathbf{x})] = \int D\rho \int D\phi \exp[-\beta(\Omega^{MF}[\phi,\rho] - \sum_{\mathbf{x}} \Delta\mu(\mathbf{x})\rho(\mathbf{x}) - \sum_{\mathbf{x}} J(\mathbf{x})\phi(\mathbf{x}))], \quad (18)$$

$$-\beta\Omega[J(\mathbf{x}),\overline{\mu}(\mathbf{x})] = \log \Xi, \quad (19)$$

where in continuum systems sums over lattice sites should be replaced by integrals $\int d\mathbf{r}$ over space positions. $-\beta\Omega[J(\mathbf{x}),\overline{\mu}(\mathbf{x})]$ is the generating functional for the (connected) correlation functions. In particular,

$$\left.\frac{\delta(-\beta\Omega)}{\delta(\beta\overline{\mu}(\mathbf{x}))}\right|_{\Delta\mu(\mathbf{x})=0} = \langle\rho(\mathbf{x})\rangle, \quad (20)$$

$$\left.\frac{\delta^2(-\beta\Omega)}{\delta(\beta\overline{\mu}(\mathbf{x}_1))\delta(\beta\overline{\mu}(\mathbf{x}_2))}\right|_{\Delta\mu(\mathbf{x})=0} = G_{\rho\rho}(\mathbf{x}_1,\mathbf{x}_2) = \langle\rho(\mathbf{x}_1)\rho(\mathbf{x}_2)\rangle - \langle\rho(\mathbf{x}_1)\rangle\langle\rho(\mathbf{x}_2)\rangle, \quad (21)$$

etc., with similar relations for the charge-density correlations. Double Legendre transform of $-\Omega[J(\mathbf{x}),\overline{\mu}(\mathbf{x})]$ is, up to minus sign, the Helmholtz free energy functional of the average OP fields,

$$\Gamma[\langle\phi\rangle,\langle\rho\rangle] = \Omega + \sum_{\mathbf{x}} J(\mathbf{x})\langle\phi(\mathbf{x})\rangle + \sum_{\mathbf{x}} \overline{\mu}(\mathbf{x})\langle\rho(\mathbf{x})\rangle. \quad (22)$$

The high-temperature, disordered phase is at the boundary of stability when the matrix of second functional derivatives of Γ is no longer positive definite.

Γ is the generating functional for the vertex functions [23]. Expanding about the values of the average OP $\langle\phi\rangle = 0$ and $\langle\rho\rangle = \rho_0$ we obtain

$$\Gamma[\overline{\phi},\overline{\rho}] = \Gamma[0,\rho_0] + \sum_{\mathbf{x}} \mu\Delta\overline{\rho}(\mathbf{x}) + \frac{1}{2}\sum_{\mathbf{x}_1}\sum_{\mathbf{x}_2} C_{\phi\phi}(\mathbf{x}_1,\mathbf{x}_2)\overline{\phi}(\mathbf{x}_1)\overline{\phi}(\mathbf{x}_2) + \frac{1}{2}\sum_{\mathbf{x}_1}\sum_{\mathbf{x}_2} C_{\rho\rho}(\mathbf{x}_1,\mathbf{x}_2)\Delta\overline{\rho}(\mathbf{x}_1)\Delta\overline{\rho}(\mathbf{x}_2) + \sum_{m>1,n>2}\sum_{\mathbf{r}_1}\cdots\sum_{\mathbf{r}_{2m}} \times \sum_{\mathbf{x}_1}\cdots\sum_{\mathbf{x}_n} \frac{\Gamma_{2m,n}(\mathbf{r}_1,\ldots,\mathbf{r}_{2m},\mathbf{x}_1,\ldots,\mathbf{x}_n)}{(2m)!\,n!} \times \overline{\phi}(\mathbf{r}_1)\cdots\overline{\phi}(\mathbf{r}_{2m})\Delta\overline{\rho}(\mathbf{x}_1)\cdots\Delta\overline{\rho}(\mathbf{x}_n), \quad (23)$$

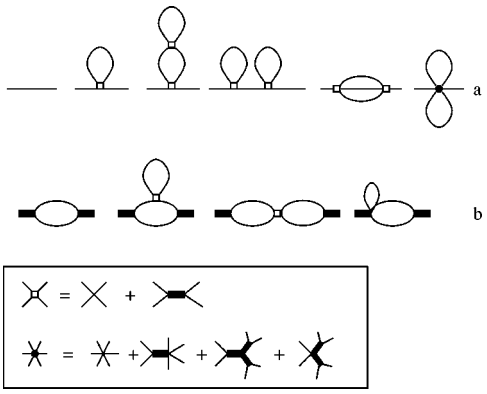

FIG. 1. Feynman diagrams contributing to the nonlocal (i.e., with $\mathbf{x}_1 \neq \mathbf{x}_2$) parts of the correlation functions, $G_{\phi\phi}(\mathbf{x}_1-\mathbf{x}_2)$ (a) and $G_{\rho\rho}(\mathbf{x}_1-\mathbf{x}_2)$ (b), up to two-loop order. Thin line connecting points $\mathbf{x}_1$ and $\mathbf{x}_2$ represents $G^0_{\phi\phi}(\mathbf{x}_1-\mathbf{x}_2)$ and the black box represents $G^0_{\rho\rho}(\mathbf{x}_1-\mathbf{x}_2) = \delta(\mathbf{x}_1-\mathbf{x}_2)G^0_{\rho\rho}$. The open square and the bullet represent the four- and the six-point hypervertices $-\mathcal{A}_4$ and $-\mathcal{A}_6$, respectively. In the inset the vertices $\gamma_{2m,n}$ contributing to the hypervertices $\mathcal{A}_4$ (top) and $\mathcal{A}_6$ (bottom) are shown. The corresponding expressions for $\mathcal{A}_4$ and $\mathcal{A}_6$ are given in Eqs. (28) and (29), respectively. Note that since with each vertex a summation (integration) over space positions is associated, the same holds for hypervertices.

where we have simplified the notation by introducing $\overline{\phi} = \langle\phi\rangle$, $\overline{\rho} = \langle\rho\rangle$, and $\Delta\overline{\rho}(\mathbf{x}) = \overline{\rho} - \rho_0$. The vertex functions in Eq. (23) are calculated at $\overline{\phi} = 0$, $\overline{\rho} = \rho_0$. The two-point vertex functions, $C_{\phi\phi}$ and $C_{\rho\rho}$ are inverse to the full correlation functions, $\tilde{G}_{\phi\phi}(\mathbf{k})$ and $\tilde{G}_{\rho\rho}(\mathbf{k})$, respectively.

In MF the vertex functions $\Gamma_{2m,n}$ reduce to $\gamma_{2m,n}$, and the correlation functions reduce to $G^0_{\phi\phi}$ and $G^0_{\rho\rho}$ when all $\gamma_{2m,n}$ are neglected in Eq. (12), i.e., in the Gaussian approximation. In the perturbation theory $C_{\phi\phi}$, $C_{\rho\rho}$ and $\Gamma_{2m,n}$ are given by appropriate one-particle irreducible Feynman diagrams according to standard rules [23]. In these diagrams there are several types of vertices $\gamma_{2m,n}$ and two types of lines, corresponding to the Gaussian correlation functions $G^0_{\phi\phi}$ and $G^0_{\rho\rho}$ [see Eqs. (13) and (14)]. The lines representing

$$G^0_{\rho\rho}(\mathbf{x}_1,\mathbf{x}_2) = G^0_{\rho\rho}\delta(\mathbf{x}_1-\mathbf{x}_2), \quad (24)$$

are degenerate in the sense that they do not connect different points. In the above $\delta(\mathbf{x}_1-\mathbf{x}_2)$ represents the Kronecker and the Dirac delta function on the lattice and in continuum, respectively. For $\sigma/a = 1$ $G^0_{\rho\rho} = \rho_0(1-\rho_0)$, and in general it is a positive function of ρ_0. From the vertex $\gamma_{2m,n}$ there emanate $2m$ "charge" lines representing $G^0_{\phi\phi}$ and n "density" lines representing $G^0_{\rho\rho}$. Finally, with each vertex $\gamma_{2m,n}$ at $\mathbf{x}$ a summation (integration) over space positions $\mathbf{x}$ is associated.

The diagrams representing nonlocal parts (i.e., with $\mathbf{x}_1 \neq \mathbf{x}_2$) of the two correlation functions, $G_{\phi\phi}(\mathbf{x}_1,\mathbf{x}_2)$ and $G_{\rho\rho}(\mathbf{x}_1,\mathbf{x}_2)$, are shown in Fig. 1 up to two loop order, when the vertices $\gamma_{2m,n}$ that satisfy $m+n \leqslant 3$ are included. By inspection of Fig. 1 one easily sees that the number density fluctuations at different points, not correlated at the zero-loop level [see Eq. (24)], become correlated beyond MF. This

leads to the conclusion that in the RPM the charge-density correlations have to be included in the lowest-order theory.

B. WEIGHTED-FIELD APPROXIMATION

In order to develop a simplest field theory which for ionic systems would predict a qualitatively correct phase diagram, recall that in MF the average densities are approximated by the most probable ones. For the RPM we follow this idea and we approximate the number density by its most probable value, but we do so for each charge-density fluctuation $\phi(\mathbf{x})$ separately, obtaining $\rho_m[\phi]$. The average number density in this theory is obtained by averaging the most probable density $\rho_m[\phi]$ over all charge-density fluctuations (therefore we call it "weighted field" (WF)). The grand thermodynamic potential in the WF approximation has the form

$$-\beta\Omega^{WF}[0,\mu] = \log\,\Xi^{WF}[0,\mu],$$

$$\Xi^{WF}[0,\mu] = \int D\phi\, \exp(-\beta\Omega_{eff}[\phi]), \tag{25}$$

where $\Omega_{eff}[\phi]=\Omega^{MF}[\phi,\rho_m[\phi]]$. In this approximation $\overline{\rho}=\langle\rho_m[\phi]\rangle_{WF}$, where $\langle\cdots\rangle_{WF}$ denotes averaging with the Boltzmann factor $\propto\exp(-\beta\Omega_{eff}[\phi])$.

For the particular case of $\sigma/a=1$ we find $\rho_m[\phi]$ from $\delta\Omega^{MF}/\delta\rho=0$ and using $\beta\mu=-\log(1-\rho_0)+\log(\rho_0/2)$ we obtain

$$\overline{\rho}(\mathbf{x}) = \rho_0 + \frac{\rho_0(1-\rho_0)}{2\rho_0-1}\sum_{n=1}\left(\frac{2\rho_0-1}{2\rho_0^2}\right)^n\frac{(2n-3)!!}{n!} \times\langle\phi^{2n}(\mathbf{x})\rangle_{WF}\ (\mathrm{sc}). \tag{26}$$

Here and in the sequel (sc) indicates that the formula corresponds only to the sc lattice with $\sigma/a=1$.

The functional $\Omega_{eff}[\phi]$ can be expanded about $\phi=0$,

$$\Omega_{eff}[\phi] = \frac{1}{2}\sum_{\mathbf{x}}\sum_{\mathbf{x}'} C^0_{\phi\phi}(\mathbf{x}-\mathbf{x}')\phi(\mathbf{x})\phi(\mathbf{x}') + \sum_{\mathbf{x}}\left[\frac{\mathcal{A}_4}{4!}\phi(\mathbf{x})^4 + \frac{\mathcal{A}_6}{6!}\phi(\mathbf{x})^6 + \cdots\right]. \tag{27}$$

The coupling constants $\mathcal{A}_4$ and $\mathcal{A}_6$ are represented by the hyper-vertices shown in the inset in Fig. 1, and are expressed in terms of the vertices $\gamma_{2m,n}$ as follows:

$$\mathcal{A}_4 = \gamma_{4,0} - 3\frac{(-\gamma_{2,1})^2}{C^0_{\rho\rho}}, \tag{28}$$

$$\mathcal{A}_6 = \gamma_{6,0} - 15\frac{(-\gamma_{2,1})(-\gamma_{4,1})}{C^0_{\rho\rho}} - 15\frac{(-\gamma_{2,1})^3(-\gamma_{0,3})}{C^{03}_{\rho\rho}} - 45\frac{(-\gamma_{2,2})(-\gamma_{2,1})^2}{C^{02}_{\rho\rho}}, \tag{29}$$

where the numerical factors have been calculated according to standard rules [23]. For $\sigma/a=1$ the explicit expressions for the coupling constants are

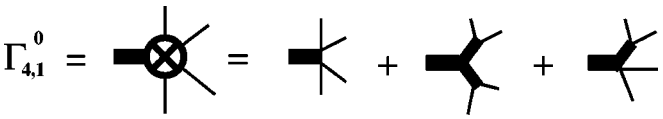

FIG. 2. The vertices $\gamma_{2m,n}$ with $m+n\leq 3$ contributing to the hypervertex $\Gamma^0_{4,1}$.

$$\mathcal{A}_4 = \frac{3\rho_0-1}{\rho_0^3}\quad(\mathrm{sc}), \tag{30}$$

$$\mathcal{A}_6 = \frac{3(3-15\rho_0+20\rho_0^2)}{\rho_0^5}\quad(\mathrm{sc}). \tag{31}$$

Note that $\mathcal{A}_4>0$ only for $\rho_0>1/3$. As already shown in Ref. [13], for $\rho_0<1/3$ the order-disorder transition becomes first order. $\mathcal{A}_6>0$ for $0\leq\rho_0\leq 1$, and the truncated functional (27) is stable for $\phi\to\infty$. From the viewpoint of stability we can thus truncate the functional at the term $\propto\phi^6$. In the perturbation theory described in the previous subsection it means that we can limit ourselves to the vertices $\gamma_{2m,n}$ with $m+n\leq 3$.

When the functional (25) is truncated, then in a consistent approximation we truncate the expansion of $\overline{\rho}$ at the term proportional to $\langle\phi^4(\mathbf{x})\rangle_{WF}$, so that in the diagrammatic expansion of $\overline{\rho}$ only vertices $\gamma_{2m,n}$ with $m+n\leq 3$ are included. In this approximation we obtain

$$\overline{\rho} = \rho_0 - \frac{\gamma_{2,1}}{2C^0_{\rho\rho}}\langle\phi^2(\mathbf{x})\rangle_{WF} - \frac{\Gamma^0_{4,1}}{4!\,C^0_{\rho\rho}}\langle\phi^4(\mathbf{x})\rangle_{WF}, \tag{32}$$

where the hypervertex $\Gamma^0_{4,1}$, obtained by standard rules [23], is given by (see Fig. 2)

$$\Gamma^0_{4,1} = \gamma_{4,1} - \frac{6(-\gamma_{2,2})(-\gamma_{2,1})}{C^0_{\rho\rho}} - \frac{3(-\gamma_{3,0})(-\gamma_{2,1})^2}{C^{02}_{\rho\rho}}. \tag{33}$$

In the particular case of $\sigma/a=1$ the average density in this approximation is explicitly given by

$$\overline{\rho} = \rho_0 + \frac{1-\rho_0}{2\rho_0}\left(\langle\phi^2(\mathbf{x})\rangle_{WF} + \frac{2\rho_0-1}{4\rho_0^2}\langle\phi^4(\mathbf{x})\rangle_{WF}\right)\quad(\mathrm{sc}). \tag{34}$$

In this work we focus on the transition to the charge-ordered phase, where $\langle\phi\rangle\neq 0$. The instability with respect to charge-ordering is given by $\tilde{C}_{\phi\phi}(\mathbf{k}_b)=0$, where $\tilde{C}_{\phi\phi}(\mathbf{k})$ is inverse to the full correlation function. In our WF theory we shall consider the approximate form $\tilde{C}^{WF}_{\phi\phi}(\mathbf{k})=\tilde{G}^{WF-1}_{\phi\phi}(\mathbf{k})$, with

$$\tilde{G}^{WF}_{\phi\phi}(\mathbf{k}) = \langle\tilde{\phi}(\mathbf{k})\tilde{\phi}(-\mathbf{k})\rangle_{WF}. \tag{35}$$

The main assumption here is that the instability of the uniform phase is induced by the charge-density fluctuations $\phi(\mathbf{x})$. We also take into account the most probable number-density fluctuations $\rho_m[\phi]$ accompanying them. Remaining number-density fluctuations are neglected.

IV. ORDER OF THE TRANSITION TO THE CHARGE-ORDERED PHASE

The field theory for the system in which the instability is induced by fluctuations characterized by $\mathbf{k}_b \neq 0$ has been developed by Brazovskii [19], and subsequently used by others for a description of various systems, including microemulsions [24] and block copolymers [25]. When the integral

$$\mathcal{G}_0 = \int_{\mathbf{k}} \tilde{G}^0_{\phi\phi}(\mathbf{k}) \tag{36}$$

representing the loop in the second diagram in Fig. 1(a) diverges at the MF line of instability $S=S_\lambda^{MF}$ [where $\tilde{C}^0_{\phi\phi}(\mathbf{k}_b)=0$], then the equation $\tilde{C}_{\phi\phi}(\mathbf{k}_b)=0$ has no solutions for finite temperatures. Instead, a first-order transition is found.

The integrand $\tilde{G}^0_{\phi\phi}(\mathbf{k})$ can be written in the form [see Eqs. (13) and (17)]

$$\tilde{G}^0_{\phi\phi}(\mathbf{k}) = \frac{T^E}{S + \tilde{V}(\mathbf{k})} = \frac{T^E}{\tau^0 + \Delta\tilde{V}(\mathbf{k})}, \tag{37}$$

where the critical parameter is defined by

$$\tau^0 = S - S_\lambda^{MF}, \tag{38}$$

S and S_λ^{MF} are given in Eq. (17), and $\Delta\tilde{V}(\mathbf{k})=\tilde{V}(\mathbf{k})-\tilde{V}(\mathbf{k}_b)$. $\mathcal{G}_0$ is infinite in continuum, on the fcc lattice and in model I [16], whereas it is finite for $\sigma/a=1$ and for model III ($\mathbf{k}_b$ are isolated vectors), so the Brazovskii argument does not apply for the latter models. Simulations, however, show continuous and first-order phase transitions in the first and in the second case, respectively [3]. The only qualitative difference between model III and the sc lattice with $\sigma/a=1$ concerns the location of the bifurcation vectors $\mathbf{k}_b$. For model III the bifurcation vectors $k_b(\pm1,\pm1,\pm1)$ are located inside the $\mathbf{k}$ domain, whereas at the sc lattice they form the vertices $\pi(\pm1,\pm1,\pm1)$ of the cube $-\pi\leqslant k_i\leqslant\pi$. In order to see the effect of the location of the bifurcation vectors, we shall define new fields by shifting $\tilde{\phi}(\mathbf{k})$, so that the critical wave vector for each shifted field $\tilde{\psi}^{(n)}(\mathbf{q})=\tilde{\phi}(\mathbf{q}+\mathbf{k}_b^{(n)})$, is $\mathbf{q}=\mathbf{0}$. The original field, critical for 8 wave vectors $\mathbf{k}_b^{(n)}$, will be replaced by several fields, some of them being critical, and the functional will assume a different form. The advantage is the fact that the functionals of several fields with the critical wave vector $\mathbf{q}=\mathbf{0}$ have been studied already [26–29], and we can apply the known methods to our particular case. In determining the order of the transition we shall limit ourselves to $\mathcal{A}_4>0$, where MF predicts a continuous transition.

1. sc lattice with $\sigma/a=1$: Bifurcation vectors at the domain boundary

Let us focus first on the sc lattice. We divide the domain $-\pi\leqslant k_i\leqslant\pi$ into different parts in such a way that for each k_i we split $[-\pi,\pi]$ into $[-\pi,-\pi/2]\cup[-\pi/2,\pi/2]\cup[\pi/2,\pi]$. Then we consider new fields defined on the new domain $\mathcal{D}$, such that $\mathbf{q}\in\mathcal{D}$ if $-\pi/2\leqslant q_i\leqslant\pi/2$. The full and the new domain are shown in Fig. 3 and 4 respectively in the case of $d=2$. The first new field, $\tilde{\psi}_1(\mathbf{q})=\tilde{\phi}(\mathbf{q})$, is just the original field for $\mathbf{q}\in\mathcal{D}$ [see Fig. 4(a)]. For the original fluctuations with the wave vectors located outside the new domain we define new fields just by shifting the arguments, namely,

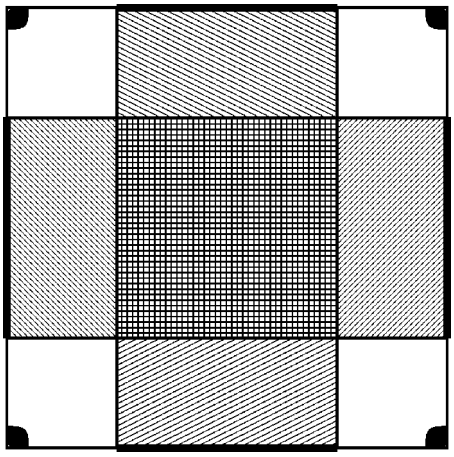

FIG. 3. The full $\mathbf{k}$ domain in the case of a two-dimensional system and the way it is divided into different parts. The central, shaded square is the new domain $\mathcal{D}$. The wave vectors with one coordinate outside $\mathcal{D}$ belong to the gray rectangles. The critical fluctuations are shown as black regions near the corners.

$$\tilde{\chi}_i(\mathbf{q}) = \tilde{\phi}(\mathbf{q}\pm\pi\mathbf{e}_i), \tag{39}$$

where $+\pi\mathbf{e}_i$ and $-\pi\mathbf{e}_i$ corresponds to $q_i<0$ and $q_i>0$ respectively. These three fields describe fluctuations with one coordinate outside the new domain. The fields $\tilde{\chi}_i(\mathbf{q})$ are defined at the whole domain $\mathcal{D}$ [see Figs. 4(b) and 4(c) for the case $d=2$]. Next,

$$\tilde{\xi}_i(\mathbf{q}) = \tilde{\phi}(\mathbf{q}\pm\pi\mathbf{e}_j\pm\pi\mathbf{e}_k), \tag{40}$$

where $i\neq j,k$ and $j<k$, and where, as above, $+\pi\mathbf{e}_n$ and $-\pi\mathbf{e}_n$ corresponds to $q_n<0$ and $q_n>0$ respectively, with $n=j,k$. These three fields describe the fluctuations with two coordinates of the wave vector outside the new domain. Again, the fields are defined at the whole domain $\mathcal{D}$. Finally, we define the field corresponding to fluctuations with all the coordinates outside the new domain,

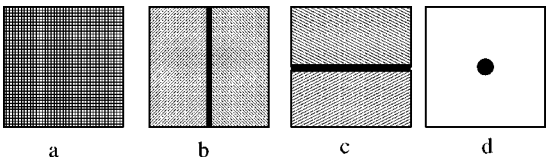

FIG. 4. Reduction of the original domain to the $\mathbf{q}$ domain $\mathcal{D}$ for the new fields, obtained by shifting the original field $\tilde{\phi}(\mathbf{k})$ in the case of a two-dimensional system: (a) the first new field is just the original field for wave vectors $\mathbf{k}$ belonging to $\mathcal{D}$; (b) and (c) the new fields $\tilde{\chi}_i(\mathbf{q})$ correspond to the original field with one coordinate of the wave vectors $\mathbf{k}$ outside $\mathcal{D}$. The thick vertical (b) and horizontal (c) lines represent the corresponding lines in Fig. 3 (d) the critical field $\tilde{\psi}_b(\mathbf{q})$ corresponds to the field $\tilde{\phi}(\mathbf{k})$ for the wave vectors $\mathbf{k}$ with all coordinates outside $\mathcal{D}$. Note that the critical regions located near the corners in Fig. 3 form here a circle centered at $\mathbf{q}=\mathbf{0}$.

$$\tilde{\psi}_b(\mathbf{q}) = \tilde{\phi}(\mathbf{q} \pm \pi\mathbf{e}_1 \pm \pi\mathbf{e}_2 \pm \pi\mathbf{e}_3), \tag{41}$$

where $+\pi\mathbf{e}_n$ and $-\pi\mathbf{e}_n$ corresponds to $q_n<0$ and $q_n>0$ respectively, with $n=1,2,3$. Note that the critical fluctuations $\tilde{\phi}(\mathbf{k}_b)$ with $\mathbf{k}_b=(\pm\pi,\pm\pi,\pm\pi)$ are all included in the last field $\tilde{\psi}_b(0)$ [for $d=2$ this case is shown in Fig. 4(d), where the central black circle represents the critical fluctuations, located at the corners in Fig. 3]. The fields ψ_1, χ_i and ξ_i are noncritical, since they correspond to the field $\tilde{\phi}(\mathbf{k})$ with $\mathbf{k}$ far from the critical vector $\mathbf{k}_b$. The functional Ω can now be written in terms of the new fields, with the integration in $\mathbf{k}$ space reduced to the new domain. The Gaussian part Ω_2^r of the new functional Ω^r can be written as

$$\beta\Omega_2^r[\Psi_n,\psi_b] = \frac{1}{2}\left(\frac{\pi\beta^E}{36}\right)\int_{\mathbf{q}\in D}[\tilde{\psi}_b(\mathbf{q})\tilde{\psi}_b(-\mathbf{q})(t_0+q^2) + \sum_{n=1}^{7} A_{\Psi_n}(\mathbf{q})\tilde{\Psi}_n(-\mathbf{q})\tilde{\Psi}_n(\mathbf{q})], \tag{42}$$

where $t_0=36\tau^0/\pi$, with τ^0 defined in Eq. (38), $q=|\mathbf{q}|$ and terms $O(q^4)$ have been neglected. Ψ_n denote all the noncritical fields ψ_1, χ_i and ξ_i defined above and $A_{\Psi_n}(\mathbf{q})$ never vanish. Only the field $\tilde{\psi}_b(\mathbf{q})$ is critical at $t_0=0$ for $q=0$. In MF the instability of the disordered phase is induced at $t_0=0$ by $\tilde{\psi}_b(\mathbf{0})$ with $\tilde{\Psi}_n=0$. The dominant higher-order term is of the usual, ψ_b^4 form for vanishing noncritical fields. The noncritical fields can be integrated out, leading to the same form of the functional of the critical field, with modified parameters [28]. We have thus reduced the functional to the standard form of the Ising universality class. The deviation of S from the value corresponding to the MF transition, $\tau_0=S-S_\lambda^{MF}$, plays analogous role as the reduced temperature in the Ising-like systems. The above reduction proves that on the sc lattice the transition to the charge-ordered phase is continuous for $\mathcal{A}_4>0$ and belongs to the Ising universality class.

2. $\sigma/a=2$ (model III): Bifurcation vectors inside the domain

In this case we again divide the $\mathbf{k}$ domain into different parts. The above analysis indicates that the fields obtained from $\tilde{\phi}(\mathbf{k})$, with $\mathbf{k}$ located far from $\mathbf{k}_b$, are noncritical and in the first approximation can be disregarded. If the bifurcation vectors are located inside the domain, however, there exists a sphere $\mathcal{S}$, which is contained in the domain $-\pi\leqslant k_i\leqslant\pi$ and centered at the critical mode $\mathbf{k}_b$. We consider $\mathbf{k}_b$ located far from the domain boundaries and the radius of the sphere $\mathcal{S}$ described above is finite. Similar case has been studied in Ref. [29] in the context of microemulsions. If there are n bifurcation (or critical) vectors, there are n different critical fields, namely

$$\tilde{\psi}_i(\mathbf{q}) = \tilde{\phi}(\mathbf{k}_b^{(i)}+\mathbf{q}), \tag{43}$$

where $\mathbf{k}_b^{(i)}$ denotes the ith bifurcation vector, and $\tilde{\psi}_i(\mathbf{q})$ is defined in the sphere $\mathcal{S}$ centered at the vector $\mathbf{k}_b^{(i)}$, i.e., $\mathbf{k}_b^{(i)}+\mathbf{q}$ belongs to the domain $-\pi\leqslant k_i\leqslant\pi$. In the critical region we can study the functional Ω of the new critical fields $\tilde{\psi}_i(\mathbf{q})$. For model III there are 8 bifurcation vectors, $\mathbf{k}_b=k_b(\pm1,\pm1,\pm1)$, where $k_b\approx\pi/4$. We can divide the bifurcation vectors into two groups. To the first group belong the bifurcation vectors with the third coordinate positive, i.e., we have $k_b(\alpha,\beta,1)$, where $\alpha,\beta=\pm1$. There are 4 such vectors, $\mathbf{k}_b^{(1)}=k_b(1,1,1)$, $\mathbf{k}_b^{(2)}=k_b(-1,-1,1)$, $\mathbf{k}_b^{(3)}=k_b(-1,1,1)$ and $\mathbf{k}_b^{(4)}=k_b(1,-1,1)$. The vectors in the second group, $k_b(\alpha,\beta,-1)$, are $-\mathbf{k}_b^{(1)}$, $-\mathbf{k}_b^{(2)}$, $-\mathbf{k}_b^{(3)}$, $-\mathbf{k}_b^{(4)}$. We shall denote the fields associated with the first group of bifurcation vectors as

$$\tilde{\psi}_i^+(\mathbf{q}) = \tilde{\phi}(\mathbf{k}_b^{(i)}+\mathbf{q}), \quad i=1,2,3,4 \tag{44}$$

and the remaining fields as

$$\tilde{\psi}_i^-(\mathbf{q}) = \tilde{\phi}(-\mathbf{k}_b^{(i)}+\mathbf{q}), \quad i=1,2,3,4. \tag{45}$$

Since $\tilde{\phi}^*(\mathbf{k}_b^i+\mathbf{q})=\tilde{\phi}(-\mathbf{k}_b^i-\mathbf{q})$ [reality condition for $\phi(\mathbf{x})$], we have $\tilde{\psi}_i^{+*}(\mathbf{q})=\tilde{\psi}_i^-(-\mathbf{q})$. In real-space representation we obtain complex fields

$$\psi_i^+(\mathbf{x}) = \int_{\mathbf{q}\in S}\tilde{\psi}_i^+(\mathbf{q})e^{-i\mathbf{q}\cdot\mathbf{x}} \tag{46}$$

and

$$\psi_i^-(\mathbf{x}) = \int_{\mathbf{q}\in S}\tilde{\psi}_i^-(\mathbf{q})e^{-i\mathbf{q}\cdot\mathbf{x}}, \tag{47}$$

where the integration is over $\mathcal{S}$. Note that $\psi_i^-(\mathbf{x})$ is a complex conjugate to $\psi_i^+(\mathbf{x})$, hence $\psi_i^\pm(\mathbf{x})=\Phi_i(\mathbf{x})\pm i\Psi_i(\mathbf{x})$, where $\Phi_i(\mathbf{x})$ and $\Psi_i(\mathbf{x})$ are real.

Let us write the Gaussian part of Ω in terms of the new fields. Since we are interested only in the stability of the disordered phase, the integral over the full domain in $\mathbf{k}$ space, $\int_{\mathbf{k}}$, can be replaced by the sum of integrals over the 8 spheres $\mathcal{S}$ centered at the 8 vectors $\mathbf{k}_b^{(n)}$, since the contribution from the neighborhood of each bifurcation vector is included, and the contributions from the noncritical fields can be neglected. Hence,

$$\int_{\mathbf{k}}\tilde{\phi}(\mathbf{k})\tilde{C}_{\phi\phi}(\mathbf{k})\tilde{\phi}(-\mathbf{k}) \tag{48}$$

can be replaced by

$$2\int_{\mathbf{q}}\sum_{i=1}^{4}\tilde{C}_i(\mathbf{q})\tilde{\psi}_i^+(\mathbf{q})\tilde{\psi}_i^-(-\mathbf{q}) = 2\int_{\mathbf{q}}\sum_{i=1}^{4}\tilde{C}_i(\mathbf{q})[\tilde{\Phi}_i(\mathbf{q})\tilde{\Phi}_i(-\mathbf{q}) + \tilde{\Psi}_i(\mathbf{q})\tilde{\Psi}_i(-\mathbf{q})], \tag{49}$$

when the stability of the uniform phase is studied. Near each bifurcation vector $\tilde{C}_{\phi\phi}(\mathbf{k})=\tilde{C}_{\phi\phi}(\pm\mathbf{k}_b^{(i)}+\mathbf{q})=\tilde{C}_i(\mathbf{q})\equiv\tilde{C}_{\alpha\beta}(\mathbf{q})$,

where in model III the i-th vector $\mathbf{k}_b^{(i)}=k_b(\alpha,\beta,1)$ corresponds to the pair $\alpha,\beta=\pm 1$. We have

$$\tilde{C}_{\alpha\beta}(\mathbf{q}) = \tau^0 + \frac{1}{2}[Aq^2 + B(\alpha\beta q_1 q_2 + \alpha q_1 q_3 + \beta q_2 q_3)] = \tau^0 + q^2 f_{\alpha,\beta}(\theta,\phi), \tag{50}$$

where $\mathbf{q}=(q_1,q_2,q_3)$, $q=|\mathbf{q}|$, and $A=\partial^2\tilde{V}/\partial k_i^2|_{|k_i|=k_b}$, $B=|\partial^2\tilde{V}/\partial k_i\partial k_j|_{|k_i|=|k_j|=k_b,i\neq j}$. On the right-hand side (RHS) $\tilde{C}_{\alpha\beta}(\mathbf{q})$ is written in spherical variables. The form of $\tilde{C}_i(\mathbf{q})$ is different for different i. However, all the fields Φ_i and Ψ_i are critical for the same thermodynamic state $\tau^0=0$ for $q\to 0$. By a suitable change of variables we can show that for any integer $k\int_{\mathbf{q}}\tilde{C}_i^k(\mathbf{q})=\int_{\mathbf{q}}\tilde{C}_1^k(\mathbf{q})$; the above holds in particular for $k=-2$.

The fourth order term can be written as

$$\Omega_{int} = \frac{A_4}{4!}\int_{\mathbf{k}_1}\int_{\mathbf{k}_2}\int_{\mathbf{k}_3}\int_{\mathbf{k}_4}\delta\left(\sum_{i=1}^4\mathbf{k}_i\right)\prod_{j=1}^4\tilde{\phi}(\mathbf{k}_j) = \frac{\mathcal{A}_4}{4!}\int_{\mathbf{q}_1}\int_{\mathbf{q}_2}\int_{\mathbf{q}_3}\int_{\mathbf{q}_4}\sum_{i,j,k,n=1}^4\tilde{\psi}_i^{\pm}(\mathbf{q}_1)\tilde{\psi}_j^{\pm}(\mathbf{q}_2)\tilde{\psi}_k^{\pm}(\mathbf{q}_3)\tilde{\psi}_n^{\pm}(\mathbf{q}_4)\delta(\pm\mathbf{k}_b^i\pm\mathbf{k}_b^j\pm\mathbf{k}_b^k\pm\mathbf{k}_b^n+\sum_{i=1}^4\mathbf{q}_i). \tag{51}$$

The above symbolic notation means 2^4 terms, associated with different distributions of $\pm$ sign for each (i,j,k,n). As before, the contributions from the noncritical modes have been neglected. Since we consider a small domain $\mathcal{S}$, the equality $\pm\mathbf{k}_b^i\pm\mathbf{k}_b^j\pm\mathbf{k}_b^k\pm\mathbf{k}_b^n+\Sigma_{i=1}^4\mathbf{q}_i=0$ can be satisfied only for $\pm\mathbf{k}_b^i\pm\mathbf{k}_b^j\pm\mathbf{k}_b^k\pm\mathbf{k}_b^n=0$. After some combinatorics we obtain

$$\Omega_{int} = \frac{A_4}{4!}\int_{\mathbf{q}_1}\int_{\mathbf{q}_2}\int_{\mathbf{q}_3}\int_{\mathbf{q}_4}\delta\left(\sum_{i=1}^4\mathbf{q}_i\right)[6\sum_{i=1}^4\tilde{\psi}_i^+(\mathbf{q}_1)\tilde{\psi}_i^+(\mathbf{q}_2)\tilde{\psi}_i^-(\mathbf{q}_3)\tilde{\psi}_i^-(\mathbf{q}_4) + 4!\sum\sum_{i<j}\tilde{\psi}_i^+(\mathbf{q}_1)\tilde{\psi}_i^-(\mathbf{q}_2)\tilde{\psi}_j^+(\mathbf{q}_3)\tilde{\psi}_j^-(\mathbf{q}_4) + 4!(\tilde{\psi}_1^+(\mathbf{q}_1)\tilde{\psi}_2^+(\mathbf{q}_2)\tilde{\psi}_3^-(\mathbf{q}_3)\tilde{\psi}_4^-(\mathbf{q}_4) + \tilde{\psi}_1^-(\mathbf{q}_1)\tilde{\psi}_2^-(\mathbf{q}_2)\tilde{\psi}_3^+(\mathbf{q}_3)\tilde{\psi}_4^+(\mathbf{q}_4))]. \tag{52}$$

In real-space representation

$$\Omega_{int} = \sum_{\mathbf{x}}[u_1^0\sum_i(\Phi_i^2(\mathbf{x})+\Psi_i^2(\mathbf{x}))^2 + u_2^0\sum_{i<j}(\Phi_i^2(\mathbf{x})+\Psi_i^2(\mathbf{x}))(\Phi_j^2(\mathbf{x})+\Psi_j^2(\mathbf{x})) + u_3^0(\Phi_1(\mathbf{x})\Phi_2(\mathbf{x})\Phi_3(\mathbf{x})\Phi_4(\mathbf{x}) + \Psi_1(\mathbf{x})\Psi_2(\mathbf{x})\Psi_3(\mathbf{x})\Psi_4(\mathbf{x}) + \Phi_1(\mathbf{x})\Psi_2(\mathbf{x})\Phi_3(\mathbf{x})\Psi_4(\mathbf{x}) + \Phi_1(\mathbf{x})\Psi_2(\mathbf{x})\Psi_3(\mathbf{x})\Phi_4(\mathbf{x}) + \Psi_1(\mathbf{x})\Phi_2(\mathbf{x})\Psi_3(\mathbf{x})\Phi_4(\mathbf{x}) + \Psi_1(\mathbf{x})\Phi_2(\mathbf{x})\Phi_3(\mathbf{x})\Psi_4(\mathbf{x}) - \Psi_1(\mathbf{x})\Psi_2(\mathbf{x})\Phi_3(\mathbf{x})\Phi_4(\mathbf{x}) - \Phi_1(\mathbf{x})\Phi_2(\mathbf{x})\Psi_3(\mathbf{x})\Psi_4(\mathbf{x}))] \tag{53}$$

where

$$u_1^0=\frac{\mathcal{A}_4}{4},\quad u_2^0=\mathcal{A}_4,\quad u_3^0=2\mathcal{A}_4. \tag{54}$$

The functional (53) is similar to the functional obtained for type II antiferromagnets in Ref. [26], and studied within ϵ expansion in Ref. [27]. Note also that the form of the functional is independent of the explicit form of $\mathcal{A}_4$, i.e. on the form of F_{hs} in Eq. (8).

Here we find the RG flow equations for the renormalized couplings u_i, determine the fixed points and show that they are all unstable. We use the standard method of dimensional regularization and minimal subtraction of pole terms in $\epsilon=4-d$ [23,30]. To one-loop order we obtain the RG flow equations

$$\ell\frac{d\overline{u_i}(\ell)}{d\ell}=\beta_{u_i}[\overline{u_j}(\ell)],\quad \overline{u_i}(1)=u_i, \tag{55}$$

$$\beta_{u_i}=\mu\partial_\mu u_i|_{u_0}=-\epsilon u_i + a_{nj}^{(i)}u_n u_j. \tag{56}$$

Here μ is the arbitrary "momentum" (i.e., the inverse length) scale, and $|_{u_0}$ means derivative at fixed bare couplings u_i^0. Equations (55) describe the flow of the renormalized couplings under rescaling the "momentum,", $\overline{\mu}(\ell)=\mu\ell$. The critical region corresponds to $\ell\to 0$. To one-loop order the dimensionless renormalized coupling constants are related to the bare quantities by [23,30]

$$u_i^0=\mathcal{K}^{-1}\mu^\epsilon\left[u_i+\frac{a_{nj}^{(i)}}{\epsilon}u_n u_j\right]. \tag{57}$$

Here $\int_{\mathbf{q}}\tilde{C}_{\alpha\beta}^{-2}(\mathbf{q})=\mu^{-\epsilon}\mathcal{K}/\epsilon$ in $4-\epsilon$ dimensions. The factors $a_{nj}^{(i)}$ can be easily obtained by considering several four-point correlation functions for the fields Φ_i,Ψ_i, and to one-loop order the explicit forms of the β-functions are

$$\beta_{u_1}=-\epsilon u_1 + 40u_1^2 + 6u_2^2, \tag{58}$$

$$\beta_{u_2}=-\epsilon u_2 + 16u_2^2 + u_3^2 + 32u_1u_2, \tag{59}$$

$$\beta_{u_3} = -\epsilon u_3 + 24 u_2 u_3. \tag{60}$$

There are four fixed points of the flow equations:

$$\text{(I)} \quad u_1^* = u_2^* = u_3^* = 0, \tag{61}$$

$$\text{(II)} \quad u_1^* = \frac{\epsilon}{40}, \quad u_2^* = u_3^* = 0, \tag{62}$$

$$\text{(III)} \quad u_1^* = \frac{\epsilon}{64}, \quad u_2^* = \frac{\epsilon}{32}, \quad u_3^* = 0, \tag{63}$$

$$\text{(IV)} \quad u_1^* = \frac{3\epsilon}{128}, \quad u_2^* = \frac{\epsilon}{64}, \quad u_3^* = 0. \tag{64}$$

For the coupling u_3 we obtain, at fixed $u_1 = u_1^*$, $u_2 = u_2^*$, the flow

$$\overline{u_3}(\ell) = u_3 \exp(\omega_3^* \log \ell), \tag{65}$$

where $\omega_3^* = -\epsilon + 24 u_2^*$ is negative for all the fixed points. Thus, for $\ell \to 0$, $|\overline{u_3}(\ell)|$ increases, which means that all the fixed points are unstable in the direction u_3. This indicates the fluctuation-induced first-order transition [27], as observed in simulations [3]. Note that on the RG flow diagram there are fixed points stable on the plane and on the axis. However, the bare copling constants are not independent [see Eq. (54)], hence stability in a subspace of the space of couplig constants does not change our conclusion.

The functional obtained for model III is not complete in the sense that the Hamiltonian with an eight-component OP in general possesses six independent coupling constants associated with six fourth-order interactions [26]. In Coulomb systems, however, there is a single fourth-order term $\mathcal{A}_4$ in the effective functional (27). Therefore, the complete Hamiltonian derived in Ref. [26] is reduced to the Hamiltonian describing model III when the coupling constants u_i^0 are related to $\mathcal{A}_4$ according to Eq. (54) for $i \leqslant 3$ and for $i > 3$, $u_i^0 = 0$. The β-functions and the fixed points obtained for the general model in Ref. [27] reduce to Eqs. (58)–(60) (and Eqs. (61)–(64), respectively, if for $i > 3$, $u_i \equiv 0$. We could assume that our model corresponds to the complete model with a special choice of the bare coupling constants (54) in the six-dimensional coupling-constants space. As shown in Ref. [27], all the fixed points in the general model are unstable to one-loop order, and we again obtain a first-order transition.

For models as complex as the considered one the one-loop results cannot be considered as fully reliable. For example, the cubic model with the real N-component OP after 30 years of intensive studies has been proved to belong to the cubic universality class [31–34]. We cannot exclude the possibility that a stable fixed-point emerges beyond the one-loop order. However, higher-order RG approximations, used in Refs. [31–34], go beyond the scope of this work. We believe that the fixed points remain unstable beyond the one-loop approximation, because simulations show a first-order transition.

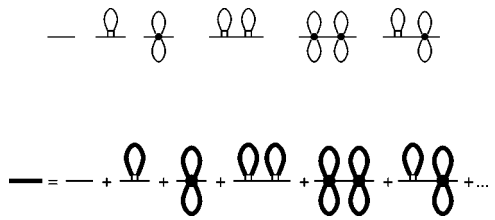

FIG. 5. Top: a few diagrams contributing to the charge-charge correlation function in the Hartree approximation. Bottom: Diagrammatic representation of the self-consistent equation for the charge-charge correlation function. The thick line represents the correlation function $\tilde{G}_{\phi\phi}(\mathbf{k})$, thin line is the Gaussian correlation function $\tilde{G}^0_{\phi\phi}(\mathbf{k})$, the box and the bullet represent the hypervertices $-\mathcal{A}_4$ and $-\mathcal{A}_6$, respectively, and the $\mathbf{k}$ integral is associated with each loop (see also Fig. 1).

V. THE λ-LINE ON THE SC LATTICE BEYOND MF

The purpose of this section is a determination of the fluctuation-induced shift of the λ-line for $\sigma/a = 1$. In MF the transition is continuous for $\mathcal{A}_4 > 0$, i.e. for $\rho_0 > 1/3$, with $\rho_0 = 1/3$ at the TCP. We shall find the temperature in the self-consistent Hartree approximation, and the density in the approximation developed here in Sec. III. In our approximation the TCP is given by the corresponding shift of the MF result.

In the Hartree approximation the correlation function is given by an infinite series of effectively one-loop diagrams, shown in Fig. 5 (top). In Fourier representation a single loop in Fig. 5 corresponds to the integral (36) and other diagrams are products of $\mathcal{G}_0$. The self-consistent approximation is obtained, when in Eq. (36) the integrand is replaced by the correlation function which is the result of the whole resummation (Fig. 5, bottom). The resulting equation is then solved self-consistently. In the self-consistent Hartree approximation, discussed in more detail, e.g., in Refs. [24,25], the $\mathbf{k}$-dependence of the correlation function is the same as given in Eq. (37), and only the critical parameter τ_0 is rescaled. Diagrams other than that shown in Fig. 5 (bottom) would lead to a change of the $\mathbf{k}$-dependent part of $\tilde{G}_{\phi\phi}(\mathbf{k})$. However, due to the divergence of $\tilde{G}^0_{\phi\phi}(\mathbf{k}_b)$ for $S = S_\lambda^{MF}$, the diagrams shown in Fig. 5 (bottom) give the dominant contribution to $\tilde{G}_{\phi\phi}(\mathbf{k})$ near the line of instability [19,24,25]. We denote the $\mathbf{k}$-integral of $\tilde{G}_{\phi\phi}(\mathbf{k})$ by $\mathcal{G}(\tau)$, and the rescaled critical parameter by τ [i.e., in this approximation $\tilde{C}_{\phi\phi}(\mathbf{k}) = \tau + \Delta\tilde{V}(\mathbf{k})$]. The self-consistent equation for $\tilde{G}_{\phi\phi}(\mathbf{k})$ assumes the form (see Fig. 5)

$$\tilde{G}_{\phi\phi}(\mathbf{k}) = \tilde{G}^0_{\phi\phi}(\mathbf{k}) \sum_{n=0} \left[-\left(\frac{\mathcal{A}_4}{2} \mathcal{G}(\tau) + \frac{\mathcal{A}_6}{2^3} \mathcal{G}^2(\tau) \right) \tilde{G}^0_{\phi\phi}(\mathbf{k}) \right]^n$$
$$= \left[\tilde{G}^{0-1}_{\phi\phi}(\mathbf{k}) + \mathcal{G}(\tau) \left(\frac{\mathcal{A}_4}{2} + \frac{\mathcal{A}_6}{2^3} \mathcal{G}(\tau) \right) \right]^{-1}. \tag{66}$$

From Eq. (66) we obtain the explicit form of the λ-line $\tilde{C}_{\phi\phi}(\mathbf{k}_b) = \tau = 0$,

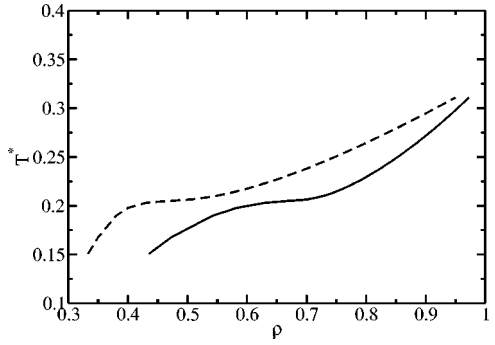

FIG. 6. The λ line in the self-consistent Hartree approximation. The dashed line gives the transition temperature as a function of the most probable density, $T^*=S_\lambda(\rho_0)$ [see Eq. (69)]. The solid line $T^*=S_\lambda(\overline{\rho})$ is the transition temperature as a function of the average density $\overline{\rho}$ given in Eq. (72). Temperature is in standard reduced units ($T^*=kTD\sigma/e^2$) and the fraction of ion-occupied sites ρ is dimensionless.

$$\tau_0 + \mathcal{G}(0)\left(\frac{\mathcal{A}_4}{2} + \frac{\mathcal{A}_6}{2^3}\mathcal{G}(0)\right) = 0. \tag{67}$$

On the sc lattice the form of $\mathcal{G}(0)$ is [see Eqs. (37) and (2) and the Appendix]

$$\mathcal{G}(0) = T^E g_1, \quad g_1 = \frac{3}{\pi}\int_{\mathbf{k}}\left(\frac{6}{3+\sum_i \cos k_i} - 1\right) \approx 1.91. \tag{68}$$

Equation (67) can be solved easily. The explicit expression for the line of instability in the self-consistent Hartree approximation is

$$S_\lambda = \frac{2(2+\mathcal{A}_4\rho_0 g_1)\left[\sqrt{1+\frac{2\mathcal{A}_6\rho_0^2 g_1^2 S_\lambda^{MF}}{(2+\mathcal{A}_4\rho_0 g_1)^2}} - 1\right]}{\mathcal{A}_6\rho_0^2 g_1^2}. \tag{69}$$

The λ-line $S=S_\lambda(\rho_0)$ is shown in Fig. 6 as a dashed line.

As discussed in Sec. III, the average number density differs from the most probable one. We can include the effect of the charge-density fluctuations on the average number density by using Eq. (34). In the self-consistent Hartree approximation for the charge-charge correlation function we assume

$$\langle\phi^2(\mathbf{x})\rangle_{WF} = \mathcal{G}(0) = g_1 S\rho_0. \tag{70}$$

Next we assume that the four-point function is a product of two-point functions up to a numerical factor [23] (see Fig. 7),

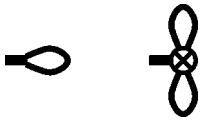

FIG. 7. The diagrams contributing to the shift of the density of ions (32) in the Hartree approximation. See also Figs. 2 and 5.

$$\langle\phi^4(\mathbf{x})\rangle_{WF} = 3\langle\phi^2(\mathbf{x})\rangle_{WF}^2, \tag{71}$$

i.e., we neglect the connected part of $\langle\Pi_i^4\phi(\mathbf{k}_i)\rangle_{WF}$, which at the zero-loop order is proportional to $-\mathcal{A}_4\Pi_i\tilde{G}^0_{\phi\phi}(\mathbf{k}_i)$ [23]. In the self-consistent Hartree approximation the two-point function in Eq. (71) is given by Eq. (70). The explicit form of $\overline{\rho}$ along the λ-line in this approximation is [see Eqs. (34), (70), and (71)]

$$\overline{\rho} = \rho_0 + \frac{g_1 S_\lambda(1-\rho_0)}{2} + \frac{3g_1^2 S_\lambda^2(2\rho_0-1)(1-\rho_0)}{8\rho_0}. \tag{72}$$

The λ-line $S_\lambda(\overline{\rho})$ given by Eqs. (69) and (72) is shown as a solid line in Fig. 6. It starts at the TCP, obtained by the corresponding shift of the TCP found in MF. Our result is compared with other theoretical and simulation results in Table I.

VI. SUMMARY

The effects of charge-density fluctuations on the order-disorder transition for different values of the space discretization σ/a have been described in Refs. [16,17]. In this work two cases, $\sigma/a=1$ and $\sigma/a=2$ have been analyzed in detail. We have shown that in both models the instability of the disordered phase is induced on the MF level by charge-density waves $\tilde{\phi}(\mathbf{k})$ with 8 wave vectors $\mathbf{k}_b^{(n)}$. However, for $\sigma/a=1$ these vectors form vertices of the cubic domain in the **k**-space, whereas for $\sigma/a=2$ they are located inside the domain, far from the boundary. For each model we constructed a functional depending on the shifted fields $\tilde{\psi}^{(n)}(\mathbf{q}) = \tilde{\phi}(\mathbf{q}+\mathbf{k}_b^{(n)})$. Next we have shown that for $\sigma/a=1$ there is only one critical field and near the line of instability of the disordered phase the functional reduces to the well known functional of the Ising-university class. Hence, the transition is continuous. In contrast, there are 8 critical fields for $\sigma/a=2$, and there is no stable fixed point of the RG-flow equations—hence a first-order transition should be expected.

On the sc lattice with $\sigma/a=1$ the instability is induced by the charge-density waves compatible with the lattice, and they all lead to a unique structure (up to $+/-$ symmetry, see Fig. 1 in Ref. [15]). The unique structure follows from the particular location of the critical wave vectors at the vertices of the cubic **k**-domain. The unique ordered structure can be easily pinpoint to the lattice and the order can grow gradually. The transition is thus continuous. Otherwise an interference of different structures associated with different wave vectors $\mathbf{k}_b^{(n)}$ restores the disordered phase. The ordered structure is not washed out by fluctuations only for a finite value of the OP, i.e., the transition is first order. The above analysis indicates that the continuous transition and the TCP are quite rare, and occur in a system with a special template.

In this work we have also developed an approximate theory allowing for a determination of quantiative effects of fluctuations. We have applied the formalism developed in Sec. III to a determination of a position of the λ-line on the sc lattice with $\sigma/a=1$. The result is shown in Fig. 6 and compared with earlier theories and simulations in Table I. At

TABLE I. Location of the TCP obtained in the MF theory [10,15], in the DH and HRT theories [20,21] and in simulations [3,4], and the result of this work. Temperature and density at the TCP in standard reduced units are denoted by T^*_{tc} and ρ^*_{tc}, respectively.

	T^*_{tc}	ρ^*_{tc}
MF [15]	0.7	1/3
MF [10]	0.299	1/3
DH [20]	0.38	0.365
HRT [21]	0.202 ± 0.002	0.38 ± 0.005
This work	0.15	0.44
Simulations [3]	0.15 ± 0.01	0.48 ± 0.02
Simulations [4]	0.14	0.4

close packing ($\hat{s}^2 \equiv 1$) we obtain $T^* \approx 0.33$ at the λ-line, which is lower than the result of simulations, $T^* \approx 0.5$ [35]. However, the weighted field theory, where number-density fluctuations are allowed, is not expected to be valid for $\rho \equiv 1$, therefore for ρ close to 1 the exact λ-line deviates from our result. In simulations the potential $1/r$ was used, and not the form we have considered for a lattice system. There are also standard sources of inaccuracy (finite system, etc.) of simulations. The position of the TCP is thus probably somewhat different. Similarly, the result of an exact theory should be somewhat different from our approximation.

The results of this and earlier works show that the theory introduced in Ref. [13] leads to qualitatively correct phase diagrams in all considered cases, including those which have not been described within any other theory (model I, model III, fcc lattice, LRPM with additional short-range forces). Moreover, the quantitative accuracy of the theory is also significantly better than the accuracy of the other theories. Clearly, further studies are necessary for a determination of phase diagrams for other values of σ/a and in continuum space on a quantitative level, but the formalism developed here seems to be particularly well suited for this purpose.

ACKNOWLEDGMENTS

The author would like to thank Professor G. Stell for inspiring suggestions, discussions, and encouragement. This work was supported by the KBN through research project 1 P02B 033 26.

APPENDIX: LATTICE COULOMB POTENTIAL

The lattice Coulomb potential is a solution of the discretized Poisson-Boltzmann equation, and in Fourier representation assumes the form

$$\tilde{V}_c(\mathbf{k}) = \frac{2\pi}{3[1 - \tilde{f}_{\mathrm{latt}}(\mathbf{k})]}, \tag{A1}$$

where the index latt denotes the sc, fcc or the bcc lattice. The lattice characteristic function $\tilde{f}_{\mathrm{latt}}(\mathbf{k})$ depends on the kind of the lattice. For the sc, fcc, and bcc lattices $\tilde{f}_{\mathrm{latt}}(\mathbf{k})$ is given by

$$\tilde{f}_{\mathrm{sc}} = \frac{1}{3}\sum_{i=1}^{3} \cos k_i, \tag{A2}$$

$$\tilde{f}_{\mathrm{fcc}}(\mathbf{k}) = \frac{1}{3}\sum_{i<j} \cos k_i \cos k_{j,} \tag{A3}$$

and

$$\tilde{f}_{\mathrm{bcc}}(\mathbf{k}) = \prod_{i=1}^{3} \cos k_i, \tag{A4}$$

respectively. The constants V_0^{sc} and V_n^{sc} are defined via equations

$$V_0^{\mathrm{sc}} = \int_{\mathbf{k}} \frac{1}{3(1 - \tilde{f}_{\mathrm{sc}}(\mathbf{k}))}, \tag{A5}$$

$$V_n^{\mathrm{sc}} = \int_{\mathbf{k}} \frac{\prod_{i=1}^{n} \cos k_i}{3(1 - \tilde{f}_{\mathrm{sc}}(\mathbf{k}))}. \tag{A6}$$

The values we need in this work are

$$V_0^{\mathrm{sc}} \approx 0.5055, \tag{A7}$$

$$V_1^{\mathrm{sc}} \approx 0.172, \quad V_2^{\mathrm{sc}} \approx 0.11, \quad V_3^{\mathrm{sc}} \approx 0.087. \tag{A8}$$

[1] M. Kleemeier, S. Wiegand, W. Schröer, and H. Weingärtner, Adv. Chem. Phys. **116**, 1 (2001); H. Weingärtner and W. Schröer, J. Chem. Phys. **110**, 3085 (1999).

[2] M. Wagner, O. Stanga, and W. Schröer, Phys. Chem. Chem. Phys. **5**, 3943 (2003).

[3] A. Z. Panagiotopoulos and S. K. Kumar, Phys. Rev. Lett. **83**, 2981 (1999).

[4] R. Dickman and G. Stell, *Treatment of Electrostatic Interactions in Computer Simulations of Condensed Media*, Proceedings of the Conference, Santa Fe, 1999, edited by G. Hummer and L. R. Pratt (AIP, Melville, NY, 1999).

[5] A. Diehl and A. Z. Panagiotopulos, J. Chem. Phys. **118**, 4993 (2003).

[6] E. Luijten, M. E. Fisher, and A. Z. Panagiotopoulos, J. Chem. Phys. **114**, 5468 (2001); Phys. Rev. Lett. **88**, 185701 (2002); A. Z. Panagiotopoulos, J. Chem. Phys. **116**, 3007 (2002).

[7] J.-M. Caillol, D. Levesque, and J.-J. Weis, J. Chem. Phys. **116**, 10794 (2002).

[8] C. Vega, J. L. F. Abascal, and C. McBride, J. Chem. Phys. **119**, 964 (2003); F. Bresme, C. Vega, and J. L. F. Abascal, Phys. Rev. Lett. **85**, 3217 (2000).

[9] G. Stell, J. Stat. Phys. **78**, 197 (1995).

[10] G. Stell, in *New Approaches to Problems in Liquid-State Theory*, edited by C. Caccamo, J.-P. Hansen, and G. Stell (Kluwer Academic, Dordrecht, 1999)
[11] M. E. Fisher, J. Stat. Phys. **75**, 1 (1994).
[12] M. E. Fisher and Y. Levin, Phys. Rev. Lett. **71**, 3826 (1993).
[13] A. Ciach and G. Stell, J. Mol. Liq. **87**, 253 (2000).
[14] A. Ciach and G. Stell, Physica A **306**, 220 (2002).
[15] A. Ciach and G. Stell, J. Chem. Phys. **114**, 3617 (2001).
[16] A. Ciach and G. Stell, Phys. Rev. Lett. **91**, 060601 (2003).
[17] A. Ciach and G. Stell, Phys. Rev. E **70**, 016114 (2004).
[18] A. Ciach and G. Stell, J. Chem. Phys. **114**, 32 (2001).
[19] S. A. Brazovskii, Sov. Phys. JETP **41**, 85 (1975).
[20] V. Kobelev, A. B. Kolomeisky, and M. E. Fisher, J. Chem. Phys. **116**, 7589 (2002).
[21] A. Brognara, A. Parola, and L. Reatto, Phys. Rev. E **65**, 066113 (2002).
[22] R. Evans, Adv. Phys. **28**, 143 (1979).
[23] D. J. Amit, *Field Theory, the Renormalization Group and Critical Phenomena* (McGraw-Hill, New York, 1978).
[24] Y. Levin, C. J. Mundy, and K. A. Dawson, Phys. Rev. A **45**, 7309 (1992).
[25] G. H. Fredrickson and E. Helfand, J. Chem. Phys. **87**, 697 (1987).
[26] D. Mukamel and S. Krinsky, Phys. Rev. B **13**, 5065 (1976).
[27] D. Mukamel and S. Krinsky, Phys. Rev. B **13**, 5078 (1976).
[28] S. Krinsky and D. Mukamel, Phys. Rev. B **16**, 2313 (1977).
[29] Y. Levin and K. A. Dawson, Phys. Rev. A **42**, 1976 (1990).
[30] H. W. Diehl, in *Phase Transitions and Critical Phenomena*, edited by C. Domb and J. L. Lebowitz (Academic, London, 1986), Vol. 10, p. 75.
[31] H. Kleinert, S. Thoms, and V. Schulte-Frohlinde, Phys. Rev. B **56**, 14428 (1997).
[32] K. B. Varnashev, Phys. Rev. B **61**, 14660 (2000).
[33] J. M. Carmona, A. Pelissetto, and E. Vicari, Phys. Rev. B **61**, 15136 (2000).
[34] R. Folk, Yu. Holovatch, and T. Yavors'kii, Phys. Rev. B **62**, 12195 (2000).
[35] N. G. Almarza and E. Enciso, Phys. Rev. E **64**, 042501 (2001).